ADVANCED MATERIALS
www.advmat.de

Surface-Energy Generator of Single-Walled Carbon Nanotubes and Usage in a Self-Powered System

By *Zheng Liu, Kaihong Zheng, Lijun Hu, Ji Liu, Caiyu Qiu, Haiqing Zhou, Haibo Huang, Haifang Yang, Meng Li, Changzhi Gu, Sishen Xie, Lijie Qiao,* and *Lianfeng Sun**

Surface energy plays an important role in surface physics,[1,2] biophysics,[3,4] surface chemistry,[5,6] and catalysis.[7] A gradient of surface energy between a solid and liquid interface can induce transport of liquids[8–11] and water running uphill,[12] which is important for DNA analysis devices.[13] Due to the 2D nature and relatively few molecules or atoms involved, the density of surface energy is usually quite small, which is impractical for utilizing surface energy as an energy source. Nevertheless it is attractive to use surface energy at the nanoscale because of the lower power consumption for nanodevices and the higher specific surface area for nanomaterials.[14–18] In this work, we demonstrate an effective design of single-walled carbon nanotubes (SWNTs) to harvest surface energy of ethanol and convert it into electricity. In this ethanol-burner-like design, an open-circuit voltage (V_{oc}) can be obtained as a result of ethanol flow in the capillary channels formed among SWNTs driven by surface tension. The V_{oc} remains constant as long as there is ethanol from the source. The maximum power can be up to ~1770 pW per device and can serve as a self-powered system to drive a thermistor. Meanwhile, the performance (the inducing rate of V_{oc}, the value of V_{oc}, and the output power) can be significantly enhanced by the Marangoni effect.[19]

SWNTs were synthesized by floating catalytic chemical vapor deposition and treated by diamond wire drawing dies,[20–22] which results in well-aligned individual SWNTs (see Supporting Information S1). The resulting SWNT rope (~25.0 mm (length) × 0.6 mm (diameter), Fig. 1a) is connected to electrodes of aluminum film, forming a suspended structure on a glass slide. The device is measured by a Keithley 4200-SCS, semiconductor characterization system, (voltage resolution 1 μV) and the dynamic characteristics of the open-circuit voltage (V_{oc}) are monitored while adding ethanol (MOS grade, 99.9%) to the beaker (Fig. 1b, see Supporting Information S2).

In an open beaker, no obvious V_{oc} is observed at the beginning (angle 40°, Fig. 2a). When the ethanol level reaches the SWNT rope, the V_{oc} begins to increase. The increase of V_{oc} is almost linear from zero to 200 μV for the first 240 s, then the V_{oc} saturates gradually at 219 μV where is remains constant over 6 h as shown in Figure 2a. V_{oc} can remain constant as long as the ethanol level is contacting the SWNT rope. When the beaker is covered as indicated by region 2 (Fig. 2b), V_{oc} will gradually decrease back to the original value. This process can be repeated

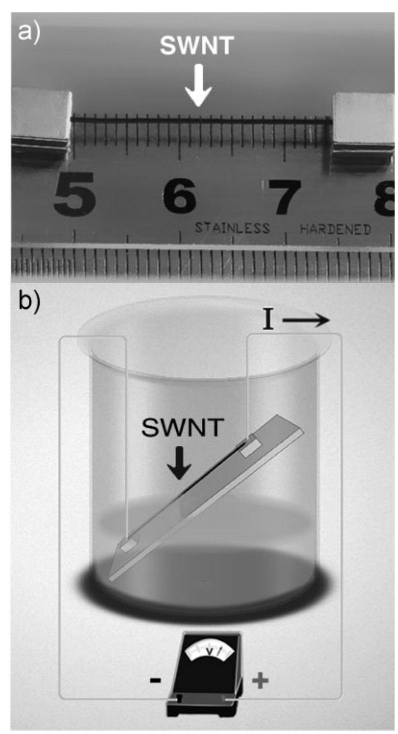

Figure 1. The SWNT device and schematic layout of the experimental setup. a) An image of the device with a suspended SWNT rope. After treating with diamond wire drawing dies, the SWNT rope has a diameter of ~0.6 mm and length of ~25.0 mm and is connected to the electrodes. b) When measuring, the device is placed into a beaker with an angle between the SWNT rope and the ethanol level. Dynamic characteristics of V_{oc} are monitored when ethanol is added into the beaker.

[*] Prof. L. F. Sun, Dr. Z. Liu, Dr. K. H. Zheng, Dr. L. J. Hu, Dr. J. Liu, Dr. C. Y. Qiu, Dr. H. Q. Zhou, Dr. H. B. Huang
National Center for Nanoscience and Technology
No. 8, Zhongguancun 1st North Street, Beijing 100190 (P.R. China)
E-mail: slf@nanoctr.cn

Prof. S. S. Xie, Prof. C. Z. Gu, Prof. H. F. Yang
Institute of Physics, Chinese Academy of Sciences
Beijing 100190 (P.R. China)

Prof. L. J. Qiao, Dr. M. Li
Corrosion and Protection Center, Key Laboratory for Environmental Fracture (MOE)
University of Science and Technology Beijing
Beijing 100083 (P.R. China)

Dr. Z. Liu, Dr. K. H. Zheng, Dr. L. J. Hu, Dr. J. Liu, Dr. C. Y. Qiu, Dr. H. Q. Zhou, Dr. H. B. Huang
Graduate School of Chinese Academy of Sciences
Beijing 100049 (P.R. China)

DOI: 10.1002/adma.200902153

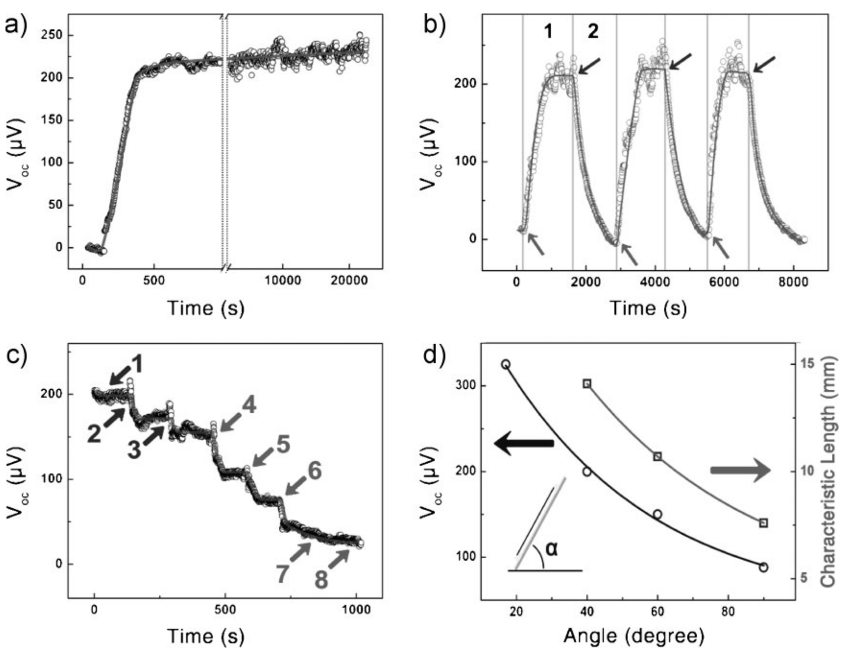

Figure 2. Dynamic characteristics of V_{oc} at $\alpha = 40^\circ$ of the SWNT rope. a) When ethanol is added into the beaker, no V_{oc} is observed until the ethanol level reaches the SWNT rope. The V_{oc} increases to a saturated value of 219 μV in about 300 s and remains constant for about 6 h. b) In an open beaker, the V_{oc} will begin to increase when the ethanol level reaches the SWNT rope and tend to a saturated value (region 1). The V_{oc} will decrease gradually back to the original value when the beaker is covered as indicated by region 2. These characteristics can be reproduced. c) When reaching the saturated value of V_{oc}, the V_{oc} does not change even if more ethanol is added (arrow 1). After certain amount of ethanol is added, the V_{oc} begins to decrease. At both points 2 and 3, 3.0 mL ethanol is added. At points 4, 5, and 6, 9.0 mL ethanol is added. At point 7, the SWNT rope is almost immersed in ethanol and no obvious change of V_{oc} is found. A similar result is obtained at point 8 when SWNT is totally immersed. According to the diameter of the beaker (68 mm) and the angle between the SWNT rope and the ethanol level (40°), the L of the SWNT rope is 14.1 mm. d) Dependence of V_{oc} and L on α of the SWNT rope. Both V_{oc} and L are closely related to α of the SWNT rope. The angles are 90°, 60°, 40°, and 17° for V_{oc} measurements. The maximum power can be up to ∼1770 pW per device (17°). L is 14.1, 10.6, and 7.6 mm for angles of 90°, 60°, 40°, respectively.

and the characteristics of varying V_{oc} can be well reproduced (Fig. 2b).

When reaching the saturated value, V_{oc} does not change until a certain amount of ethanol is added into the beaker. When 3.0 mL of ethanol is added into the beaker as indicated by the time points 2 and 3 in Figure 2c, a drop of V_{oc} (∼20 μV) is found. The addition of 9.0 mL of ethanol is carried out at points 4, 5, and 6. At this time, the ethanol level almost reaches the top electrode. The addition of ethanol does not cause an obvious change for time points 7 and 8, as shown in Figure 2c. These results suggest a characteristic length (L) for the device. When the length of the SWNT rope over the ethanol level is longer than L, the induced V_{oc} always takes the maximum value and the addition of ethanol into the beaker does not cause any change of V_{oc}. If the length of the SWNT rope over the ethanol level is equal to L, the induced V_{oc} begins to decrease with additional ethanol. The L can be calculated using $V/(\pi r^2 \sin\alpha)$, where V is the total volume of ethanol that causes changes in V_{oc}, r is the radius of the beaker, and α is the slant angle of the SWNT. The maximum V_{oc} and L are closely related to α and device-dependent. For the device reported, the relationships between V_{oc}, L and α are plotted in Figure 2d.

More interesting phenomena can be found if the SWNT rope is pretreated. Before measurements for V_{oc}, the device can be fixed where droplets of deionized water (Millipore, 18 MΩ cm^{-1}) fall on the SWNT rope. After this treatment for several minutes, the device is transferred into the beaker for further studies (Fig. 1b). When ethanol is added into the beaker and its level reaches the SWNT, a very sharp increasing of V_{oc} is observed (Fig. 3b). The V_{oc} jumps to 853 μV in less than 1 s (inset of Fig. 3b), representing a significant increasing rate compared to that in Figure 3a. The V_{oc} remains at this value for about 50 s and decreases gradually to a value of ∼223 μV, which is quite close to that when using pure ethanol (Fig. 3a).

What is the mechanism of these interesting observations? A possible electrochemical potential difference at the metal/SWNT interface for V_{oc} can be excluded for two reasons. Firstly, when ethanol level reaches the SWNT rope, a linear increasing behavior of V_{oc} is observed instead of a sharp one, which is expected if there exists an electrochemical potential difference for the faster response time of hundreds of milliseconds to several seconds (Fig. 2a).[23] Secondly, if the beaker is covered, the V_{oc} decreases to a value of nearly zero, which indicates that the electrochemical potential difference at the metal/SWNT interface is negligible.

When the ethanol level reaches the SWNT rope, surface tension pulls the ethanol molecules up along the channels formed among individual SWNTs, which have dimensions around hundreds of nanometers, because of the ethanol contact angle of ∼0° (Supporting Information, Fig. S1b and S3). The moving ethanol molecules along the SWNT can induce a V_{oc} because of the coupling between the charge carriers of the SWNTs and the flowing molecules at the interface.[22,24,25] At capillary equilibrium, however, ethanol no longer moves and hence no V_{oc} should be observed. This is in contradiction with our experimental results. Based on the device design and experimental results, we propose an ethanol-burner-like model as shown in Figure 3c and d. When ethanol molecules climb up along the channels among the SWNTs, these molecules also evaporate from the rising liquid at the same time. The average length that ethanol molecules move along the channel before they evaporate is L (Fig. 3c). When certain ethanol molecules pass L and evaporate at the top, the same quantity of ethanol will climb up along the channels among the SWNTs from the bottom. This forms a steady, dynamic, and directional ethanol flow and results in the constant V_{oc} that can be obtained as long as the SWNT rope is immersed in ethanol (Fig. 2a). L cannot be visually observed in our experiment because the SWNT rope is black whether it is wetted by ethanol or not.

Poiseuille's law can be used to estimate linear velocity of this novel ethanol laminar flow at the steady state.[26,27] The linear

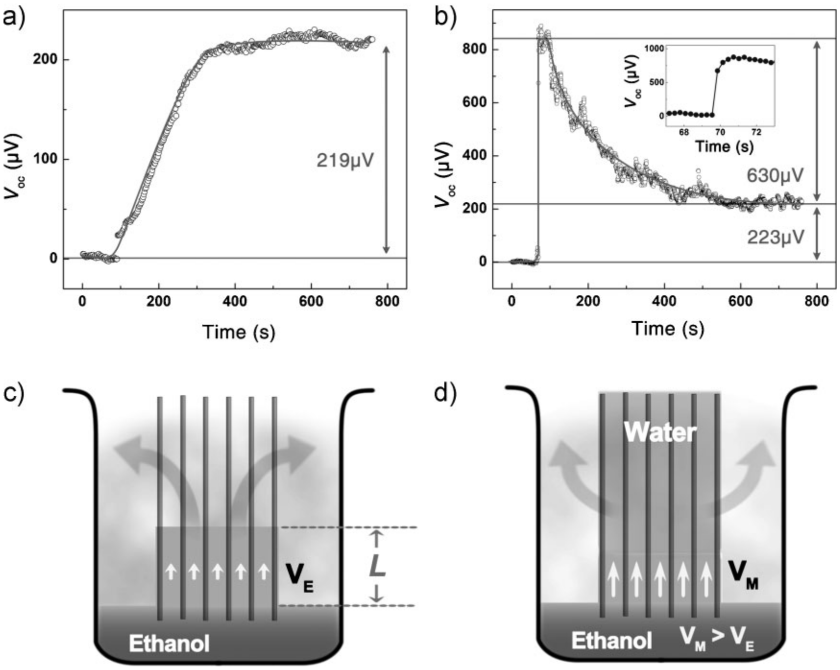

Figure 3. Comparison between the SEG and the Marangoni-enhanced SEG and diagrams showing the mechanisms. a) When the SWNT rope is immersed by ethanol, the V_{oc} increases and reaches a value of ~219 µV in about 300 s. b) Once the SWNT is pretreated with water, the V_{oc} jumps to a value of 853 µV in less than 1 s, indicating a much higher inducing rate and larger value of V_{oc} of the SEG by the Marangoni effect. Usually the V_{oc} maintains at the maximum value for tens of seconds and decreases gradually to a value similar to that of the pure ethanol SEG. c) Once the ethanol level reaches the SWNT rope, the ethanol climbs along the channels among the SWNTs due to capillary forces. These ethanol molecules evaporate after passing an average distance of L. Thus a steady capillary flow of ethanol forms as in the case of an ethanol burner. This is why a V_{oc} can be obtained as long as there is ethanol in the beaker. d) Once the SWNT is pretreated with water, the flowing velocity of ethanol is increased by the Marangoni effect. Both the inducing rate of V_{oc} and the value of V_{oc} are enhanced. The V_{oc} decreases gradually to a value similar to that for pure ethanol after the water molecules evaporate completely.

velocity of ethanol (v) can be calculated using Equation (1):

$$v = r_c^2 (P_C - P_L)/8\eta L \tag{1}$$

where η is the viscosity of the liquid, r_c is the average radius of the capillary channels, P_c is the capillary pressure difference at the ethanol level in the beaker across the interface ($2\sigma/r_c$, where σ is the surface tension), P_L is the hydrostatic pressure of liquid ($P_L = \rho g L \sin\alpha$, where ρ the density of liquid, g is the gravitational constant). The velocity of ethanol is estimated to be 57 $\mu m \cdot s^{-1}$. Therefore, the time for the ethanol to rise across L is $L/v = 14.1\,mm/(57\,\mu m \cdot s^{-1}) = 247\,s$, which is in good consistency with that found in Figure 3a.

If the beaker is covered, the evaporation of ethanol will increase the vapor pressure inside the beaker. When the vapor pressure finally reaches the saturated pressure, the dynamic, directional flow of ethanol will be stopped, and the induced V_{oc} decreases back to its original value as shown in Figure 2b.

When the length of the SWNT rope is longer than L, the added ethanol just raises the level of ethanol in the beaker and that inside the channels among the SWNTs (Fig. 3c). In this situation, no change in V_{oc} can be observed (Fig. 2c, time point 1). As a certain amount of ethanol is added and the length of SWNT rope is equal to or less than L, the V_{oc} begins to decrease because there are less moving ethanol molecules inside the channels (Fig. 2c, time points 2–6). Finally, the V_{oc} decreases to zero and does not change anymore as the ethanol level reaches the top electrode (Fig. 2c, time points 7 and 8).

If the SWNT rope is pretreated with water, as ethanol has a lower surface tension than water, the surface tension difference provides an additional driving force for the ethanol climbing up along the channels among the SWNTs, which is called the Marangoni Effect (Fig. 3d).[19,28,29] It is rather complicated to calculate the exact enhanced velocity, and the average velocity of ethanol molecules can be estimated as follows.

At present it is unclear whether L still exists when a Marangoni effect enhances the flow of ethanol. Since the induced V_{oc} is closely related to the interface area between moving ethanol molecules and SWNTs, it is reasonable to assume that when the V_{oc} reaches the maximum value, the ethanol molecules moved from the bottom electrode and reached the top electrode. From the dynamic characteristics in the inset of Figure 3b, an average velocity of ~25.0 $mm \cdot s^{-1}$ for ethanol can be obtained. Compared to the velocity of 57 $\mu m \cdot s^{-1}$ for pure ethanol, an enhanced factor of 439 for the velocity has been obtained due to the Marangoni effect.[10] The inducing rate for the observed V_{oc} is enhanced by a factor of 300, which is similar to the enhancing factor (439) of the velocity of ethanol in the pretreated ropes of SWNTs. Meanwhile, the magnitude of V_{oc} is enhanced by a factor of 3.9 for the water-pretreated SWNT ropes (the corresponding power is increased by a factor of 15). It is reasonable that the V_{oc} depends both on the velocity of ethanol and the number of ethanol molecules at the SWNT/water (or ethanol) interface, both of which vary with time. When the V_{oc} reaches its maximum value (Fig. 3b), the velocity of ethanol decreases and the number of ethanol molecules at the SWNT/water (or ethanol) interface increases. This joint effect makes the V_{oc} stable at the maximum value for tens of seconds. The V_{oc} decreases to a similar value to that of pure ethanol when the water effect disappears.

Because the flow of ethanol inside the channels is driven by surface tension, these generators are named surface-energy generators (SEGs). The electrical power of the SEGs can be estimated by

$$P = V_{oc}^2/R \tag{2}$$

where P is the electrical power, and R is the inner resistance. Values of 794 pW and 12.0 nW can be obtained for the pure-ethanol SEG and the Marangoni-enhanced SEG (angle 40°), respectively, indicating an enhancing factor of 15 for power by the Marangoni effect. The surface area of the SWNT rope contacting the ethanol can be calculated by $\pi r^2/\sin\alpha$, where r is the diameter of the SWNT rope (~0.6 mm). The optimum powers obtained are 1.8 mW and 27.3 mW per square meter for the pure-ethanol SEG and the Marangoni-enhanced SEG, respectively, which are high enough to drive nanodevices.[18] Here we demonstrate that these SEGs can be used to drive a negative-temperature-coefficient thermistor without additional power (Fig. 4 and Supporting Information, Figs. S4–6). The voltage drop across the thermistor (powered solely by the SEG) as a function of time (Fig. 4) shows a reversible increase (or decrease) as the temperature of the thermistor is decreased (or increased). These processes can be repeated and the voltage drop is consistent with the expected changes in the resistance of the thermistor (Supporting Information, Fig. S6).

Control experiments were carried out with films of SWNTs and carbon fibers. A much smaller V_{oc} is found in SWNT films, indicating that the alignment is beneficial to the formation of oriented and regular channels among the SWNTs and important for the generation of a higher V_{oc} (Supporting Information, Figs. S7 and S8) and no V_{oc} is found for carbon fibers (Supporting Information, Fig. S9). The inducing characteristics of V_{oc} have also been studied for other organic solvents, such as methanol and acetone. These solvents can also induce a V_{oc} and the V_{oc} can be enhanced by pretreating of SWNT rope with water, indicating the universality of these phenomena (Supporting Information, Fig. S10).

In summary, we demonstrate that an effective design of SWNTs can be used to convert the surface energy of liquids into electricity. The mechanism could be ascribed to the unique channels among individual SWNTs, in which a continuous, steady flux of liquid forms. The inducing rate of V_{oc}, the magnitude of V_{oc}, and the optimum output power can be significantly enhanced by the Marangoni effect. These kinds of SEGs can be used to serve as a self-powered system and have a quite different operating mechanism and show the advantages of a smaller inner resistance, a lack of moving parts, and no application of an obvious external force.

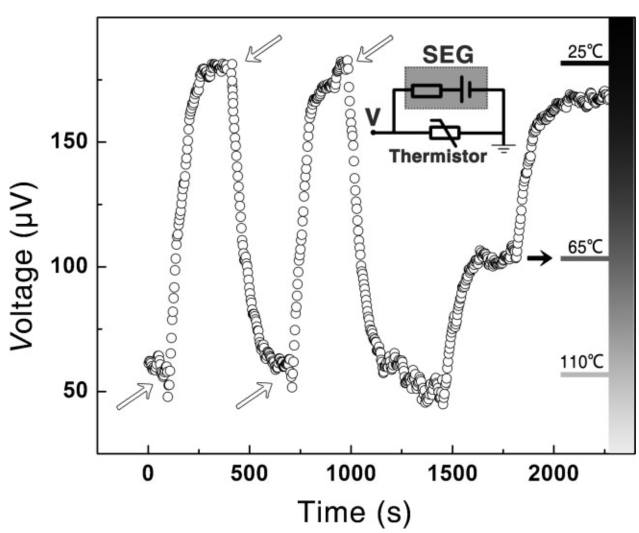

Figure 4. Self-powered system with a SEG. A negative temperature coefficient thermistor is powered by an SEG of SWNTs ($V_{oc} = 382\,\mu$V, $I_{sc} = 1.42\,\mu$A (I_{sc} is the short-circuit current), $R = 269\,\Omega$ (R is the inner resistance). The voltage drop across the thermistor is detected with varying temperature. The hollow arrows indicate the time when the temperature begins to increase or decrease. The solid arrow shows that the voltage becomes stable when temperature keeps constant at 65 °C. Inset: circuit schematic.

Experimental

SWNTs were prepared by floating catalytic chemical vapor deposition [30]. After growing for about 6 h, large-sale SWNT films with areas as large as 15 cm × 2 cm could be carefully peeled off from the inside wall of the quartz tube. Diamond wire drawing dies were used to fabricate aligned SWNT ropes as shown in the Supporting Information, Figure S1. In order to thread the SWNT films through the dies, an as-grown SWNT film was firstly immersed into deionized water. A U-shape copper wire (100-μm diameter) was then used to pull the SWNT film out of the water and thread it through the first die. The pulling processes through the other two dies are similar to the first one. For this work, the SWNT samples are treated with diamond for ~2–3 times and the density of the SWNT rope was much smaller, which was different with our previous work [20]. During the experiments, the sample was suspended on a glass slide with both ends connected to the aluminum electrodes. A Keithley S4200 was employed to monitor the induced voltage and take current–volatage (I–V) characterizations of the sample during the experiments.

Acknowledgements

Z. Liu and K. H. Zheng contributed equally to this work. This work is supported by the ''973'' Program of the Ministry of Science and Technology (2006CB932402) and the National Science Foundation of China (Grant No. 10774032,90921001). Supporting Information is available online from Wiley InterScience or from the author.

Received: June 27, 2009
Revised: September 24, 2009
Published online: January 4, 2010

[1] W. A. de Heer, *Rev. Mod. Phys.* **1993**, *65*, 611.
[2] U. Diebold, *Surf. Sci. Rep.* **2003**, *48*, 53.
[3] D. L. Hu, J. W. M. Bush, *Nature* **2005**, *437*, 733.
[4] D. L. Hu, B. Chan, J. W. M. Bush, *Nature* **2003**, *424*, 663.
[5] D. A. Tomalia, A. M. Naylor, I. William, A. Goddard, *Angew. Chem. Int. Ed.* **1990**, *29*, 138.
[6] F. Schreiber, *Prog. Surf. Sci.* **2000**, *65*, 151.
[7] B. Hammer, J. K. Nørskov, *Adv. Catal.* **2000**, *45*, 71.
[8] M. Grunze, *Science* **1999**, *283*, 41.
[9] B. S. Gallardo, V. K. Gupta, F. D. Eagerton, L. I. Jong, V. S. Craig, R. R. Shah, N. L. Abbott, *Science* **1999**, *283*, 57.
[10] S. Daniel, M. K. Chaudhury, J. C. Chen, *Science* **2001**, *291*, 633.
[11] K. Ichimura, S.-K. Oh, M. Nakagawa, *Science* **2000**, *288*, 1624.
[12] M. K. Chaudhury, G. M. Whitesides, *Science* **1992**, *256*, 1539.
[13] M. A. Burns, C. H. Mastrangelo, T. S. Sammarco, F. P. Man, J. R. Webster, B. N. Johnsons, B. Foerster, D. Jones, Y. Fields, A. R. Kaiser, D. T. Burke, *Proc. Natl. Acad. Sci. U. S. A.* **1996**, *93*, 5556.
[14] Z. L. Wang, J. H. Song, *Science* **2006**, *312*, 242.
[15] A. I. Hochbaum, R. Chen, R. D. Delgado, W. J. Liang, E. C. Garnett, M. Najarian, A. Majumdar, P. D. Yang, *Nature* **2008**, *451*, 163.
[16] Y. Qin, X. D. Wang, Z. Wang, *Nature* **2009**, *457*, 340.

[17] J. Liu, P. Fei, J. H. Song, X. D. Wang, C. S. Lao, R. Tummala, Z. L. Wang, *Nano Lett.* **2008**, *8*, 328.
[18] B. Z. Tian, X. L. Zheng, T. J. Kempa, Y. Fang, N. F. Yu, G. H. Yu, J. L. Huang, C. M. Lieber, *Nature* **2007**, *449*, 885.
[19] L. E. Scriven, C. V. Sternling, *Nature* **1960**, *187*, 186.
[20] G. T. Liu, Y. C. Zhao, K. Deng, Z. Liu, W. G. Chu, J. R. Chen, Y. L. Yang, K. H. Zheng, H. B. Huang, W. J. Ma, L. Song, H. F. Yang, C. Z. Gu, G. H. Rao, C. Wang, S. S. Xie, L. F. Sun, *Nano Lett.* **2008**, *8*, 1071.
[21] G. T. Liu, Y. C. Zhao, K. H. Zheng, Z. Liu, W. J. Ma, Y. Ren, S. S. Xie, L. F. Sun, *Nano Lett.* **2009**, *9*, 239.
[22] Y. C. Zhao, L. Song, K. Deng, Z. Liu, Z. X. Zhang, Y. L. Yang, C. Wang, H. F. Yang, A. Z. Jin, Q. Luo, C. Z. Gu, S. S. Xie, L. F. Sun, *Adv. Mater.* **2008**, *20*, 1772.
[23] B. R. Goldsmith, J. G. Coroneus, V. R. Khalap, A. A. Kane, G. A. Weiss, P. G. Collins, *Science* **2007**, *315*, 77.
[24] S. Ghosh, A. K. Sood, N. Kumar, *Science* **2003**, *299*, 1042.
[25] P. Král, M. Shapiro, *Phys. Rev. Lett.* **2001**, *86*, 131.
[26] M. Majumder, N. Chopra, R. Andrews, B. J. Hinds, *Nature* **2005**, *438*, 44.
[27] J. K. Holt, H. G. Park, Y. Wang, M. Stadermann, A. B. Artyukhin, C. P. Grigoropoulos, A. Noy, O. Bakajin, *Science* **2006**, *312*, 1034.
[28] Y. J. Cai, B.-m. Zhang Newby, *J. Am. Chem. Soc.* **2008**, *130*, 6076.
[29] A. M. Cazabat, F. Heslot, S. M. Troian, P. Carles, *Nature* **1990**, *346*, 824.
[30] W. J. Ma, L. Song, R. Yang, T. H. Zhang, Y. C. Zhao, L. F. Sun, Y. Ren, D. F. Liu, L. F. Liu, J. Shen, Z. X. Zhang, Y. J. Xiang, W. Y. Zhou, S. S. Xie, *Nano Lett.* **2007**, *7*, 2307.